npj Regenerative Medicine

https://doi.org/10.1038/s41536-026-00482-x

Article in Press

Comparison of cardiac regeneration capacity between zebrafish and medaka reveals a regenerative response in both teleost species

Received: 20 October 2025

Accepted: 3 June 2026

Published online: 01 July 2026

Cite this article as: Garitagoitia-Romero, M.A., Galardi-Castilla, M., Torres, M. *et al.* Comparison of cardiac regeneration capacity between zebrafish and medaka reveals a regenerative response in both teleost species. *npj Regen Med* (2026). https://doi.org/10.1038/s41536-026-00482-x

Miguel Angel Garitagoitia-Romero, María Galardi-Castilla, Miguel Torres & Nadia Mercader

Comparison of cardiac regeneration capacity between Zebrafish and Medaka reveals a regenerative response in both teleost species

Miguel Angel Garitagoitia-Romero[1,2], Maria Galardi-Castilla[1], Miguel Torres[1,3], Nadia Mercader[1,4,5,#]

Affiliations

[1] Centro Nacional de Investigaciones Cardiovasculares Carlos III, Madrid, Spain.
[2] Universidad Autónoma de Madrid (UAM), Escuela de doctorado, Madrid, Spain.
[3] Centro de Investigación Biomédica en Red de Enfermedades Cardiovasculares (CIBERCV), Madrid, Spain.
[4] Institute of Anatomy, University of Bern, Switzerland.
[5] Department for BioMedical Research, University of Bern, Switzerland.
[#] corresponding author

Correspondence to

Nadia Mercader

Institute of Anatomy

Baltzerstrasse 2

3012 Bern

nadia.mercader@unibe.ch

ABSTRACT

Danio rerio (Zebrafish) can regenerate their heart upon loss of over 20% of the total myocardium. A second teleost species, *Oryzias latipes* (Medaka), however, has been described to lack this capacity and respond to a lesion forming a permanent fibrotic scar after heart resection. An altered immune response has been suggested to underly the differences in heart regeneration. However, a thorough comparative analysis between Zebrafish (AB strain) and Medaka (Cab strain) through the different steps of regeneration was lacking. Here we provide an in-depth characterization of the injury response and heart regeneration in both teleost species after ventricular cryoinjury (CI). We observed an exacerbated neutrophil activation with little evidence of macrophage recruitment in Medaka compared to Zebrafish. However, cardiomyocyte proliferation significantly increased in both teleosts upon CI. We also observed transient blood vessel formation in Medaka and a significant reduction of fibrotic tissue at 30 and 60 dpi compared to 7 dpi. However, some animals presented signs of an irreversible scar at 60 dpi and ventricular indentations suggestive of impaired regeneration. Nonetheless, echocardiographic assessment revealed cardiac function recovery in a subset of Medaka, independent of the fibrotic tissue resolution. Overall, we conclude that the cardiac regenerative ability is broader in Medaka than anticipated.

Graphical Abstract.

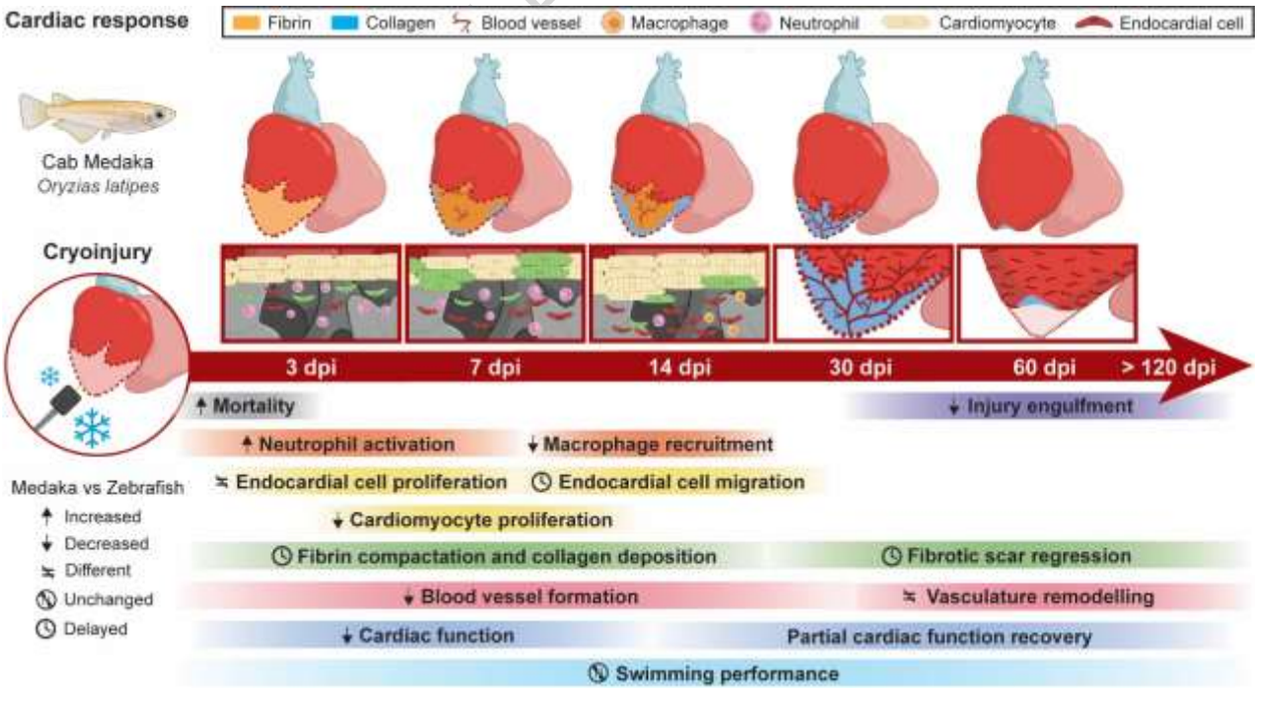

INTRODUCTION

Heart regeneration has been extensively studied in *Danio rerio* (commonly referred to as Zebrafish), and since its first description[1], there has been significant advances in the understanding of the cellular processes involved. Upon CI, there is a rapid inflammatory response leading to the infiltration of neutrophils and subsequently accumulation of macrophages into the wound[2]. This inflammatory process peaks at around 3 days postinjury (dpi) and is followed by consecutive proliferative rounds of all cardiac cells. The first cardiac cells to be activated are endocardial and epicardial cells, in which proliferation starts peaking concomitantly with the immune response at 3 dpi[3]. Epicardial and endocardial-derived cells lose their adhesions, proliferate, and migrate into the wound, forming a scaffold which will physically support the new myocardium, allow revascularization, and generate the mitogens needed for proliferation[4]. Fibroblasts accumulate at the injury site and extracellular matrix (ECM) components, mostly fibrin and collagen, are deposited forming a fibrotic plaque[5]. Simultaneously, endocardial and endothelial sprouts enter into the wound and form new coronary vessels[6]. Thereafter, cardiomyocytes in the surroundings of the injury (approximately 100 μm of the nearby ventricle) lose their sarcomeric structure[7], switch transiently from fatty acid to carbohydrate usage[8], express cell cycle progression regulators and reactivate heart developmental programs needed to undergo mitosis, being the peak of proliferation between 7 and 14 dpi. During weeks 2 to 4, the lost tissue is replaced by new myocardium, and the transiently deposited fibrotic tissue is reabsorbed[9]. Complete regeneration varies from 30 to 120 dpi and, apart from interindividual differences, it depends on the initial lesion size[10]. The recovery also occurs at the functional level. However, of note, regeneration does not totally recreate the non-injured heart[11]. The distinction between inner trabecular, intermediate primordial and outer cortical myocardial layers for example, is not fully reestablished, and the cortical layer appears thickened in the regenerated Zebrafish heart[11]. Additionally, some of the fibroblasts accumulated during the injury response remain in the regenerated heart in an inactive state[5]. Finally, while the ventricular fractional shortening is recovered, in most cases ventricular wall motion remains disturbed at the area of injury[11].

Contrary to Zebrafish, a second teleost species, *Oryzias latipes* (commonly known as Medaka), has been described to lack regenerative capacity upon cardiac ventricle resection or cryolesion[12]. However, research regarding the balance between the pro-regenerative and pro-fibrotic responses putatively found in Zebrafish and Medaka, respectively, is still at its very early stages, and research publications related to this topic are scarce. In its first characterization, no increase in cardiomyocyte proliferation could be observed after ventricular resection by 1-week EdU incorporation at either 7 or 13 days post amputation (dpa). Additionally, the collagen deposits were not reabsorbed up to 60 dpa, resulting in the formation of a permanent fibrotic scar[13]. However, the cardiac injury response initially described in Medaka[13] was based on a limited number of fish and restricted to ventricular apex resection, hence needed to be validated by other injury models. In a second seminal article, Lai *et al.*, focused on the immune response alterations in Medaka *vs* Zebrafish after a cardiac CI and found that Medaka have a delayed infiltration of macrophages and increased neutrophils activation compared to Zebrafish[14,15]. However, they did not

perform direct comparisons in proliferative or fibrotic responses between both teleost species. Finally, a third work focused on the transcriptional comparison of heart regeneration between the species at early timepoints of the CI response, but lacked a long-term quantitative analysis of the injury resolution in this species[16]. Thus, overall, there is a need for a better characterization of the response dynamics to injury between Zebrafish and Medaka, in particular regarding cardiomyocyte proliferation and fibrotic tissue regression. Furthermore, there are no functional studies on Medaka's response to CI regarding cardiac function and physical performance.

Here, we compared the response of Medaka and Zebrafish to a cardiac CI along the different stages of heart regeneration. Contrary to current perception, Medaka reproduced several of the essential hallmarks of heart regeneration in Zebrafish, including the increase in cardiomyocyte proliferation, blood vessel formation and regression of the fibrotic plaque. The dynamics of the injury response, however, differed between both teleost species, with Medaka showing a delayed immune response and fibrotic tissue remodeling compared to Zebrafish. Nevertheless, Medaka was able to regress almost completely the fibrotic plaque after injuries of up to $^1/_5$ of the ventricle, correlating in some cases with the recovery of cardiac function.

RESULTS

Medaka shows a higher mortality rate than Zebrafish in response to a cardiac CI

Medaka is more sensitive to heart resection than Zebrafish, leading to a higher mortality rate in this injury model[13]. However, quantitative data from this observation was missing. Therefore, to address the physiological impact of a cardiac CI (Figure 1a), Medaka and Zebrafish were monitored routinely before and after the procedure. Immediately after the surgery, both cryoinjured species rapidly recovered consciousness. Noticeably, Medaka's survival rate was substantially lower than that of Zebrafish, having an accumulated survival rate of 49% vs 90% over 130 days. Most of the death events took place during the first hours after surgery, and no obvious changes in fish activity or behavior could be seen for the rest of the trial. To assess if a deficient basal cardiac function could be affecting fish survival, a cohort of 28 uninjured Medaka was evaluated by echocardiography on basal conditions, and cryoinjured soon after the same day. The fish were grouped as dead or alive (survivors) for the analysis (Figure 1b-d). Only 55% of cryoinjured Medaka survived the surgery (Figure 1b). We observed a decreased fractional shortening (FS) (Figure 1c) and increased heartbeat (Figure 1d) at t_0 in the individuals that died after the CI, indicating that less efficient systolic contraction correlates with a higher mortality after a cardiac CI in Medaka. Nevertheless, the survival ratio of sham-operated Medaka was 67%, suggesting that most of the short-term mortality is already apparent after thoracotomy.

To further characterize the sensitivity to the CI procedure, Medaka were exposed to each CI step from the manipulation of the fish to the generation of the lesion (Figure 1a and e). Interestingly, even though the highest mortality rate was found in the cryoinjured group (N=3 out of 5 animals), mortality was also observed after just opening the pericardium (N=2 out of 5 animals) or performing the sham surgery (N=1

out of 5 animals). No other CI steps from the fish's manipulation to the opening of the skin and muscle produced any mortality (Figure 1e). Almost no bleeding could be observed during the surgery, and no visual signs of infection or damage in internal organs could be associated to mortality.

In conclusion, Medaka is more vulnerable to cardiac CI than Zebrafish, in particular when basal fractional shortening is lower than 10%. Nevertheless, the reasons underlying Medaka's higher sensibility to opening the pericardial sac and its associated mortality are still inconclusive and must be further studied.

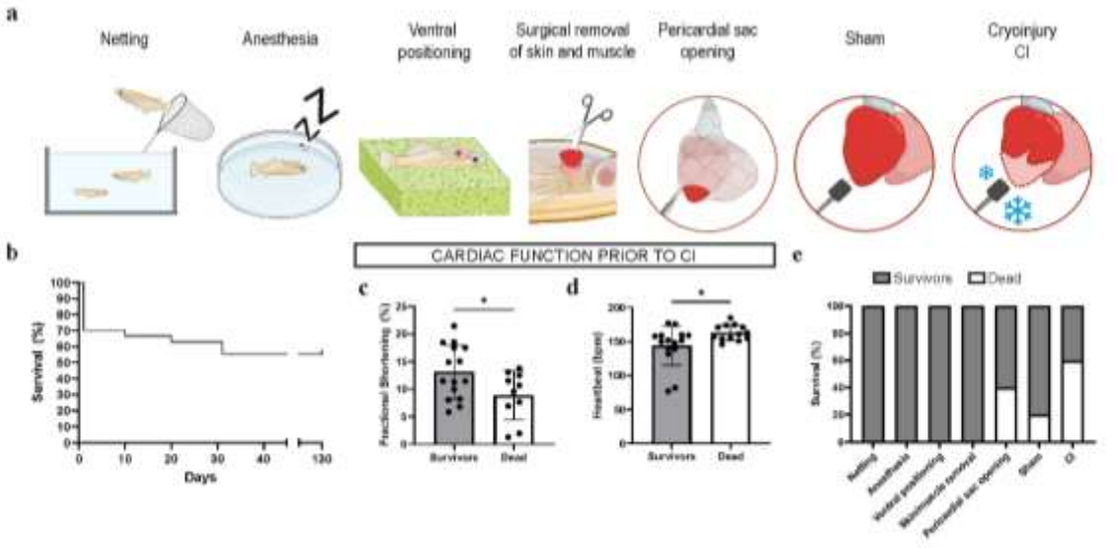

Figure 1: Survival rate after ventricular cryoinjury in Medaka.

a Graphical representation of the cryoinjury (CI) protocol. Images created with BioRender. **b** Kaplan-Meier plot of a Medaka cohort (N=28) showing survival during 130 days after cryolesion. **c and d** Quantification of fractional shortening % (c) and heartbeat bpm, beats per minute (d), of Medaka prior to CI using echocardiography. Data were divided into two groups: those that survived at 130 dpi (Survivors) and those that died after CI (Dead). Shown are measurements of individual fish as well as means ± S.D. Statistical differences were analyzed by unpaired t-test. **e** Bar plot representation of survivors (gray) versus dead (white) Medaka across the different steps of the CI procedure (N=5 per condition). *p <0.05.

The proliferative response after a cardiac CI shares similar spatiotemporal dynamics in both Zebrafish and Medaka

In order to evaluate the regenerative capacity of Medaka versus Zebrafish after CI, we first analyzed the proliferative activity of cardiac cells at 3, 7 and 14 dpi by measuring BrdU incorporation during the 24 hours prior to the extraction of the heart. Myosin Heavy Chain (MHC) and ERG immunostainings were used to identify cardiomyocytes and endocardial cells, respectively (Figure 2a) in the injury area (IA) + border zone (BZ) and the peripheral ventricular area (PA) (Figures 2b-e and Figure S1a-f).

In both species, the basal cardiomyocyte proliferation index was close to 0 (Figure 2b). However, there was an increase in response to injury at the BZ that peaked at 7 dpi and then dropped seven days later.

Nevertheless, while proliferation was increased in both species, it was significantly higher in Zebrafish than in Medaka at 7 and 14 dpi (Figure 2b). The cardiomyocyte proliferation index in the PA was mostly absent in both teleosts (<0.3% cardiomyocytes). Nevertheless, cardiomyocyte BrdU incorporation was significantly higher in Medaka than in Zebrafish in the PA at 3 dpi (Figure 2c), suggesting a broader activation of cardiomyocyte proliferation during the early cardiac CI response. We also quantified BrdU incorporation in cardiomyocytes by normalizing the amount of BrdU+ MHC+ cells per area, obtaining similar results (Figure S1a and b). The number of BrdU+ MHC+ cells in the BZ increased after injury in both species, peaking at 7 dpi and dropping to lower numbers at 14 dpi. In Zebrafish, the number of BrdU+ MHC+ cells per area was slightly higher at 7 dpi than in Medaka (Figure S1a). In Medaka, proliferation in the PA was slightly higher than in Zebrafish (Figure S1b) In conclusion, Medaka and Zebrafish both respond to a cardiac CI with induction of cardiomyocyte cell cycle, being this response higher in Zebrafish than in Medaka at the BZ and vice versa in the PA, although quantitative differences between species are moderate.

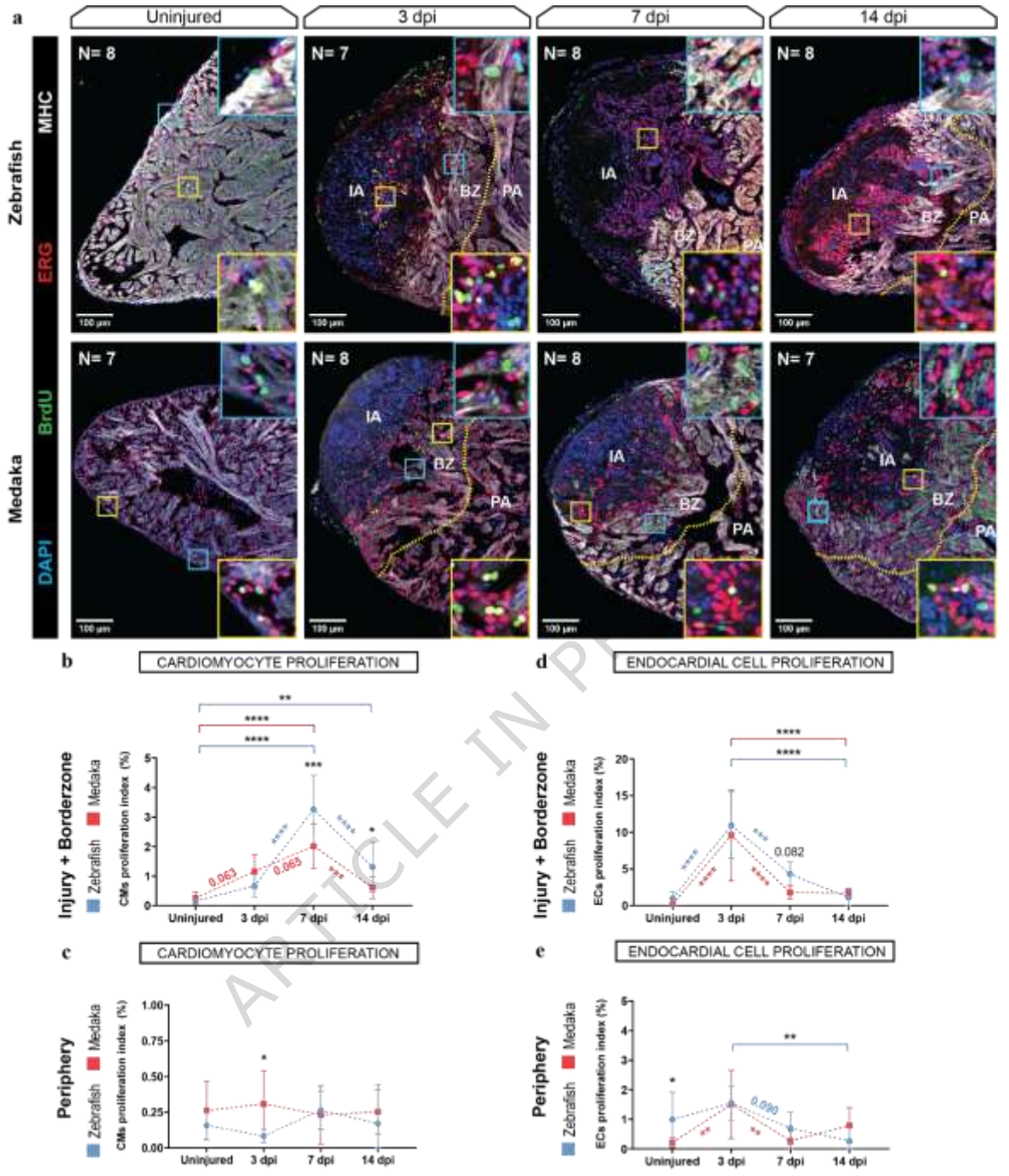

Figure 2: Spatio-temporal analysis of the proliferative response during Zebrafish and Medaka heart regeneration.

a Representative images of uninjured and cryoinjured (3, 7 and 14 dpi) Zebrafish and Medaka heart sections immunostained for BrdU (proliferation marker, green), ERG (endocardial cell marker, red), MHC (myocardium, grey) and DAPI counterstained nuclei (blue). A yellow dashed line separates the BZ, corresponding to the 100 µm myocardial area close to the IA, from the rest of ventricle, named PA. Boxes are zoomed in views highlighting BrdU+ cardiomyocytes (blue boxes) and BrdU+ endocardial cells (yellow boxes). Group sample sizes (N) and 100 µm scale bars are indicated within panels. **b-e** Quantification of cardiomyocyte MHC+ (b and c) and endocardial cell ERG+ (d and e) proliferation (BrdU+), in Zebrafish (blue) and Medaka (red) uninjured and cryoinjured (3, 7 and 14 dpi) hearts. The

number of proliferative cells is normalized by the total number of each cell type to determine the % of proliferating cells. Shown are means ± S.D. values. Statistical differences were analyzed by Two-way ANOVA with Bonferroni's correction. Significant differences between species are shown above the specific time point and differences between two time points among each species are shown by color (blue: Zebrafish; red: Medaka). p < 0.1 (number); *p <0.05; **p <0.01; ***p <0.001; ****p <0.0001. BZ, border zone; dpi, days postinjury; IA, injured area; PA, peripheral area.

Similar to cardiomyocytes, we also observed upregulation of endocardial cell (EC) proliferation after CI in both teleost species. The proliferation index at the IA+BZ increased similarly in Zebrafish and Medaka to up to 10% at 3 dpi and then dropped at 7 dpi to reach basal levels at 14 dpi (Figure 2d). In the PA, basal EC proliferation index was higher in Zebrafish than in Medaka. However, at 3 dpi, EC proliferation was similar for both species and decreased over time until 14 dpi (Figure 2e). Interestingly, while EC proliferation by area led to similar tendencies to those shown for EC proliferation index at the IA+BZ, the normalization by area showed a much more pronounced increase at the PA in Medaka than in Zebrafish (Figure S1c and d). To study how EC cells colonize the IA during regeneration, we subdivided the IA into five consecutive equidistant sections according to their BZ distance: 1 being the closest to the BZ and 5 being the apex, and quantified EC density in the distinct sections at different time points (Figure S2a). We noticed that the density of endocardial cells was much higher in Medaka than in Zebrafish both in the uninjured conditions and at the PA upon injury (Figure S2b-d). At 3 dpi, we observed endocardial cells localized in sections 1 and 2 of the IA closer to the BZ, but not in sections 3-5 in both species (Figure S2b). At 7 dpi, the amount of EC cells in Zebrafish was significantly superior to the one in Medaka in all IA sections (Figure S2c). Later, at 14 dpi, EC density was again equal in both species and equivalent among sections. Nevertheless, overall EC density in Medaka was reduced at the IA compared to the rest of the heart areas or the uninjured heart, whereby EC density was not significantly different between the different time points (Figure S2d). Our results reveal that Medaka has a higher density of EC in the adult heart and suggest that EC colonization of the IA is faster in Zebrafish than in Medaka.

Finally, BrdU incorporation in double negative non-cardiomyocyte non-endocardial cells (ERG- MHC- BrdU+ cells; rest of cells) was significantly upregulated after a CI at the IA+BZ of Zebrafish and Medaka in a similar manner, being highest at 3 dpi and decreasing over time until returning to basal levels at 14 dpi (Figure S1e). Interestingly, in Medaka the observed upregulation was not restricted to the BZ but was also observed in the PA (Figure S1f), suggesting once more a broader early proliferative response in this species.

Medaka immune response to heart CI is dominated by neutrophils with little macrophage contribution

One of the main differences between Zebrafish and Medaka cardiac injury response have been found to be associated with the immune system[14-17]. Hence, we decided to revisit immune cell infiltration in both

species adding further time points, and quantified neutrophils (Mpx+ cells) and macrophages (IB4+ cells) at 3, 7 and 14 dpi (Figure 3a). Neutrophil recruitment reached its peak in both teleost species at 3 dpi in the IA+BZ area, yet this increase was much higher in Medaka in comparison to Zebrafish. This difference between species was maintained at 7 dpi but was no longer visible at 14 dpi, when neutrophil abundance was reduced in the wound of Medaka, reaching similar levels to those in Zebrafish (Figure 3b). Interestingly, although to a lower extent than in the IA+BZ areas, neutrophils were also significantly higher in the PA of Medaka versus Zebrafish at the 3 time points post injury studied (Figure 3c), suggesting a broader activation of neutrophils after a CI in this species. Following neutrophil recruitment, macrophages invaded the wound at 7 dpi in Zebrafish, reaching similar levels in the IA+BZ to neutrophils at this stage. Number of IB4+ macrophages increased even further at 14 dpi (Figure 3d). On the contrary, IB4+ cells remained almost completely absent in Medaka, only slightly increasing at 14 dpi in both the IA+BZ (Figure 3d) and PA (Figure 3e), yet this increase was only statistically significant at the PA. Finally, no significant differences could be observed between uninjured and sham-operated Medaka, supporting that the neutrophils' and macrophage's responses observed are directly derived from the cardiac CI (Fig S3).

These data recapitulate the delay in the neutrophil clearance and reduced macrophage recruitment found before[15].

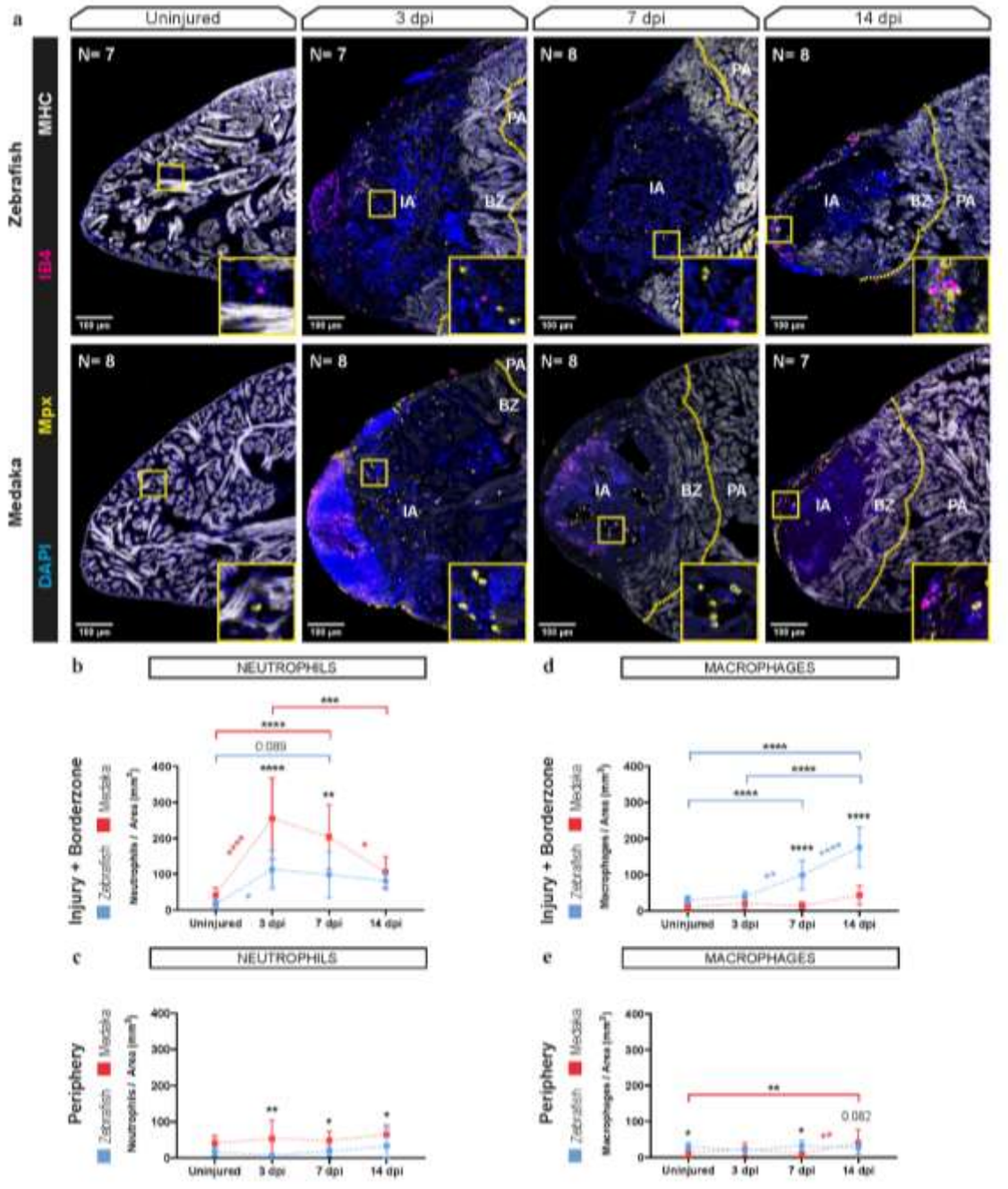

Figure 3: Spatio-temporal dynamics of the immune response after a cardiac cryoinjury in Zebrafish and Medaka.

a Representative images of uninjured and cryoinjured (3, 7 and 14 dpi) Zebrafish and Medaka heart sections immunostained for Mpx (neutrophils, yellow), IB4 (macrophages, magenta), MHC (myocardium, grey) and DAPI counterstained nuclei (blue). A yellow dashed line separates the BZ, corresponding to the 100 µm myocardial area close to the IA, from the rest of ventricle, named PA. Boxes are zoomed in images highlighting immune cell populations. Group sample sizes (N) and 100 µm scale bars are indicated within panels. **b-e** Quantification of neutrophils Mpx+ (b and c) and macrophage IB4+ (d and e) populations in Zebrafish (blue) and Medaka (red) hearts. The number of cells is normalized by area (mm^2). Shown are mean ± S.D. values. Statistical differences were analyzed by Two-way ANOVA with Bonferroni's

correction. Significant differences between species are shown above the specific time point and differences between two time points among each species are shown by color (blue: Zebrafish; red: Medaka). $p < 0.1$ (number), *p <0.05; **p <0.01; ***p <0.001; ****p<0.0001. BZ, border zone; dpi, days postinjury; IA, injured area; PA, peripheral area.

Fibrotic plaque removal is delayed, yet present in Medaka after a CI

Since cardiomyocyte proliferation was increased at 7 dpi after a CI in both Medaka and Zebrafish, we decided to analyze the fibrotic scar remodeling to further evaluate the regenerative capacity of both teleost species.

Given the high mortality rate observed in Medaka after CI, we first studied the dynamics of the fibrotic plaque remodeling by generating a small injury in Medaka. To that end, the time that the cryo-probe touched Medaka's ventricle was reduced from three to two seconds, resulting in a ≈4% smaller mean injury in Medaka (9.45%) in comparison to Zebrafish (13.6%) (Figure 4a-f). We performed Acid Fucsin Orange G (AFOG) staining on cardiac sections at 7, 14, 30 and 60 dpi. The fibrotic plaque area was significantly reduced in Zebrafish at 14 dpi and kept decreasing until only about 1.9% of the ventricular area was formed by fibrotic tissue at 60 dpi (Figure 4b). In Medaka the fibrotic plaque remained of similar size between 7 and 14 dpi, suggesting a delay in fibrotic tissue regression in this species. However, the fibrotic plaque was significantly decreased at later time points until only about 1% of the ventricle was formed by collagen at 60 dpi (Figure 4e). Wound closure could be observed in both teleost species. Yet, despite the smaller initial injury, less than 50% of Medaka revealed complete closure, while the majority of Zebrafish hearts presented a closed wound region (Figure 4c and f). Thus, while wound closure is reduced in Medaka, significant fibrotic tissue regression occurs in both teleost species when a small injury is induced.

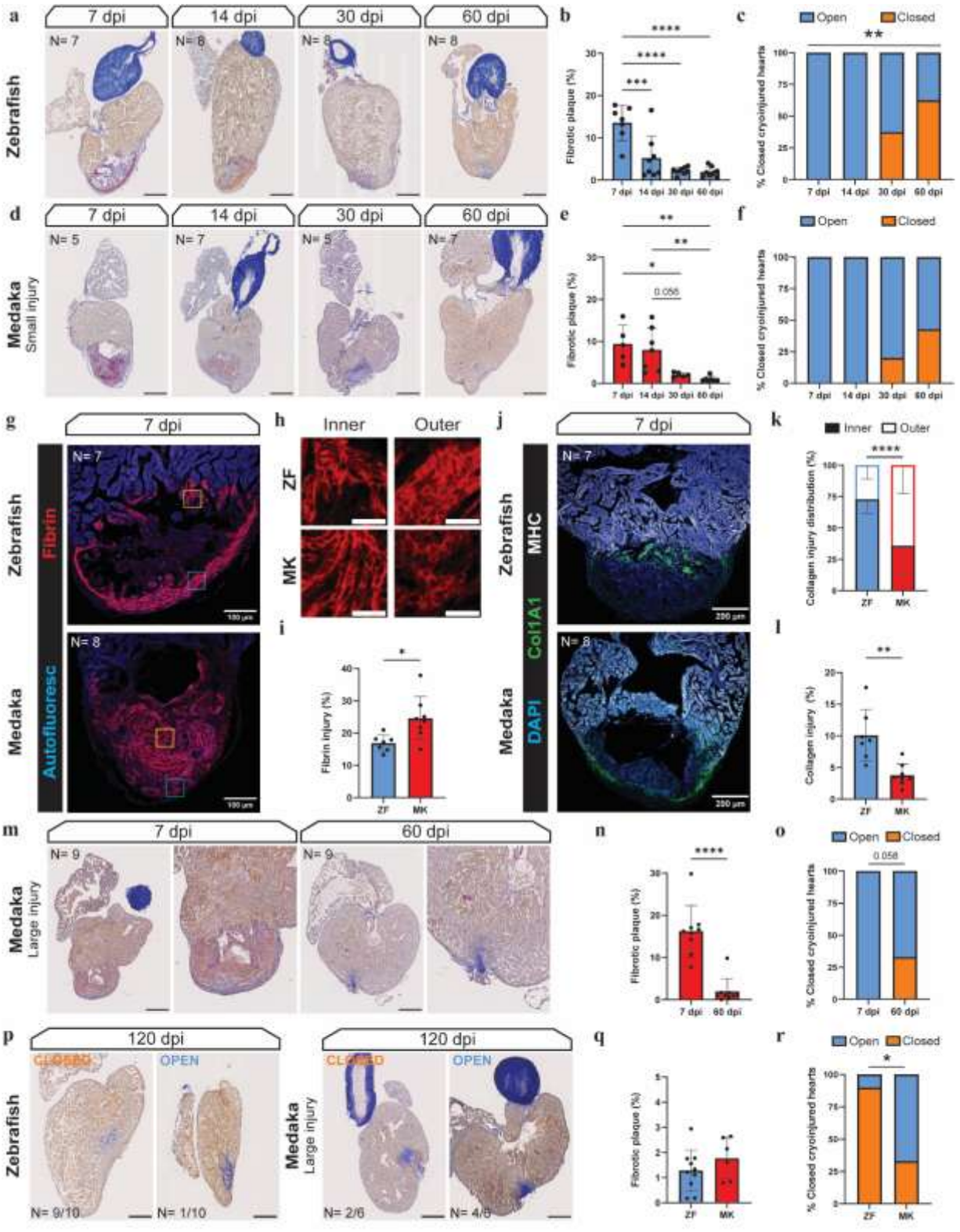

Figure 4: Fibrotic tissue deposition and regression during Zebrafish and Medaka heart regeneration

a-f Quantification of fibrosis on histological stainings of hearts at 7, 14, 30 and 60 dpi of Zebrafish (a-c) or Medaka small injury (d-f). **a and d** Representative AFOG-stained heart sections (blue: collagen, orange: fibrin, brown: myocardium). Scale bars, 250 µm. **b and e** Quantification of the percentage of fibrotic plaque vs whole ventricle area (%) in Zebrafish (b) and Medaka (small injury) (e) at the different

time points. One-way ANOVA with Bonferroni's correction. **c and f** Bar plot representation of open (blue) versus closed (orange) hearts (%) at 7, 14, 30 and 60 dpi in cryoinjured Zebrafish (c) and small-CI Medaka (f). Chi-square test. No significant differences could be found in (f). **g** Representative confocal microscope images of AFOG-stained Zebrafish and Medaka heart sections at 7 dpi. Shown is fibrin (red) and tissue autofluorescence (blue). Boxes mark inner (yellow) and outer (blue) fibrin areas of the injury zoomed in (h). Scale bars, 100 µm. **h** Zoomed-in confocal images of the inner and outer fibrin areas of Zebrafish and Medaka IA shown in (g). Shown is fibrin (red). Scale bars, 20 µm. **i)** Quantification of the fibrin area as a percentage of the IA at 7 dpi. Unpaired t-test. **j** Representative images of Zebrafish and Medaka 7 dpi heart sections immunostained for Col1A1 (collagen 1A1, green), MHC (myocardium, grey) and DAPI counterstained nuclei (blue). Scale bars, 200 µm. **k** Quantification of the collagen distribution assessed by stainings shown in (j) and distinguishing between the inner (colored bar) and outer (outlined bar) areas of the injury. Two-Way ANOVA. **l** Collagen area quantification (%) at 7 dpi. Unpaired t-test. **m** Similar to (d) but for large-CI Medaka hearts at 7 and 60 dpi, including zoomed in views of the IA. **n** Fibrotic plaque quantification (%) in large-CI Medaka whole hearts at 7 and 60 dpi. Unpaired t-test. **o** Bar plot representation of open (blue) versus closed (orange) hearts (%) at 7 and 60 dpi in large-CI Medaka. Chi-square test. **p** Representative AFOG-stained heart sections of closed (left) and open (right) Zebrafish and large-CI Medaka at 120 dpi. Scale bars, 250 µm. **q** Fibrotic plaque quantification (%) in whole hearts at 120 dpi for both species. Unpaired t-test. No significant differences could be found. **r** Bar plot representation of open (blue) versus closed (orange) hearts (%) at 120 dpi in both species. Chi-square test. Group sample sizes (N) are indicated in all panels. $p < 0.1$ (number); *$p < 0.05$; **$p < 0.01$; ***$p < 0.001$; ****$p < 0.0001$. dpi, days postinjury; MK; Medaka, ZF; Zebrafish.

We also detected differences in the early accumulation of fibrin and collagen between Zebrafish and Medaka at 7 and 14 dpi. In Zebrafish, fibrin fibers were packed around the outer part of the injury and collagen was mainly deposited internally (Figure 4a). On the other hand, in Medaka a clump of disorganized fibrin fibers covered almost the totality of the wound and collagen deposits were mostly found in the surroundings outside of the fibrotic plaque (Figures 4d). Visualization of the AFOG-stained sections by confocal imaging revealed significant differences in the compaction of the fibrin fibers, showing a more disorganized and porous pattern in the outer injury area of Medaka and a larger increase in its total amount in comparison to Zebrafish (Figure 4g-i). Immunostaining with anti-col1a1 at 7 dpi confirmed the differences in collagen deposition observed by AFOG. While collagen fibers were mostly found in the inner border of the IA in Zebrafish, collagen 1A1 staining accumulated at the periphery in Medaka. Furthermore, at this stage, we were able to observe more col1a1 staining in Zebrafish compared to Medaka, suggesting a different pace of fibrotic response between both teleost species (Figure 4j-l).

To address if the fibrosis regression observed could also take place on bigger wounds, the fibrotic plaque remodeling after a larger injury of approximately 16% of Medaka's ventricle (Figure S4) was next

examined (Figure 4m-o). As seen previously, the fibrotic plaque was mostly formed by fibrin at 7 dpi, covering almost the totality of the wound (Figure 4m). At 60 dpi, the fibrotic plaque was nearly completely reabsorbed (Figure 4n and S4). Nevertheless, wound closure was observed in only 3/9 hearts (Figure 4o). Therefore, we decided to explore if regeneration after a large CI was complete at 120 dpi (Figure 4p). In Zebrafish, complete regeneration could be observed in 4/10 cryoinjured hearts. From the six not fully-regenerated animals, only one had an open wound with prominent accumulation of over 3% fibrotic tissue. On the other hand, only 1/6 cryoinjured hearts had almost completely regressed its fibrotic plaque in Medaka (Figure 4p). The percentage of fibrotic tissue was not significantly different between both species (Figure 4q). However, significant differences could be observed in wound closure and collagen disaggregation. The injury was closed in 9/10 Zebrafish's hearts, but definitive wound closure was only observed in 2/6 Medaka hearts (Figure 4r), and the collagen remnants appeared aggregated rather than dispersed as happened in Zebrafish.

In conclusion, Medaka is able to remove most of the fibrotic tissue after a CI. However, this process is delayed, and engulfment of the fibrotic plaque is only achieved in a smaller percentage of fish than observed for Zebrafish, which is directly dependent on the starting injury size.

The regression of the injury is supported by the formation of transient blood vessel sprouts in Medaka's heart

Revascularization of the lesion is essential for the stabilization of the regenerated myocardium in Zebrafish[6] and has been shown to be differently regulated in Medaka after a CI[15,16]. Hence, we decided to explore whether the reduction of the fibrotic plaque observed in the presented study was associated with the generation of new vessels into the IA.

Endogenous alkaline phosphatase (AP) staining was carried out in Zebrafish and Medaka whole hearts which allows the staining of superficial high-AP expressing endothelial cells (Figure S5a). As a control of blood vessel AP specificity, the gills were stained in both species (Figure S5b). While in Zebrafish we observed defined coronary vessels covering the ventricular surface, a well-structured coronary tree could not be identified in the uninjured Medaka heart, as was previously described[18]. In Zebrafish, pre-existing coronary arteries invaded the IA at 7 dpi and continued to grow and ramified until fully covering the regenerated myocardium with a microvascular network by 60 dpi. In Medaka, vessel-like structures emerged inside the IA at 7 dpi and later enlarged and extended beyond the injury border zones. At 60 dpi, most of the enlarged vessels were not visible any longer, and by 120 dpi the vascular pattern was nearly indistinguishable from the uninjured heart, being consistent with the description of a transient vascularization after CI in this teleost[13,15]. Of note, while the open wound was notably reduced on the surface of both teleost species, Medaka hearts extracted at 60 and 120 dpi exhibited a more rounded appearance and presented small invaginations in the apex (Figure 5a), suggesting that the morphology of the heart is not completely recovered. Finally, a persisting injury could still be seen in some Zebrafish (1/4) and Medaka (1/3) hearts at 120 dpi (Figure S5c), consistent with the incomplete regeneration

observed in some individuals by AFOG staining (Figure 4p-r).

To further investigate the formation of the transient blood vessel structures, Medaka and Zebrafish whole-hearts were immunostained against Podocalyxin-2 (PODXL-2), a cell surface sialomucin expressed in blood vessel endothelial cells[19]. Similar to AP stainings, coronary vessels were observed in Zebrafish, but not in Medaka hearts (Figure 5b). Three distinct regions were analyzed separately: the IA, and two consecutive borderzone areas delimited by sequential 100 µm sections from the IA towards the healthy myocardium (BZ-1 and BZ-2) (Figure 5b and c). A significant increase in PODXL-2 signal could be observed in Medaka's IA and BZ-1 at 7 dpi in comparison to the outer BZ-2 (Figure 5d). At 14 dpi, the PODXL-2+ area was significantly increased as well in the BZ-2 region in comparison to its levels at 7 dpi, forming an organized vasculature connecting the inside and outside areas of the injury in 3/6 hearts. By 60 dpi, most PODXL-2+ vessel-like structures surrounding the IA were not visible anymore and quantification revealed a statistically significant decrease in the BZ-2 compared to 14 dpi (Figure 5b and d). When comparing PODXL-2+ area between both species, we observed that this was significantly higher in the IA of Zebrafish than Medaka both at 7 and 14 dpi (Figure 5e). In sum, AP and PODXL-2 stainings at different states of Medaka injury response suggest a transient local blood vessel formation in Medaka after CI. However, while both species are capable of inducing blood vessel formation after injury, Zebrafish rely on its coronary vascular tree to colonize the IA, in contrast to Medaka, where vessel-like structures are transiently formed in the IA and its surroundings.

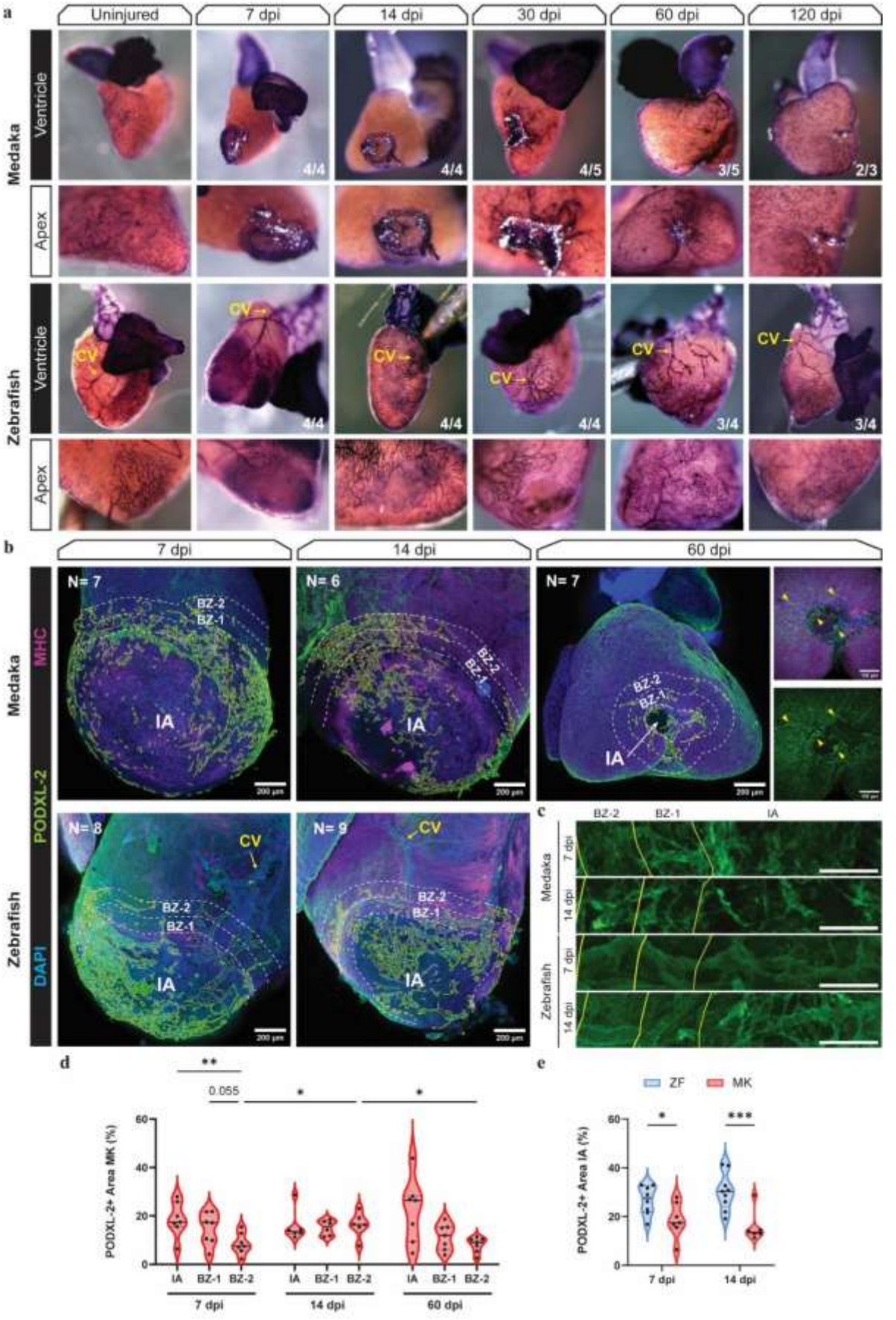
a
Uninjured
7 dpi
14 dpi
30 dpi
60 dpi
120 dpi
Medaka
Ventricle
Apex
Zebrafish
Ventricle
Apex
CV
4/4
4/4
4/5
3/5
2/3
4/4
4/4
4/4
3/4
3/4
b
7 dpi
14 dpi
60 dpi
Medaka
MHC
PODXL-2
Zebrafish
DAPI
N= 7
N= 6
N= 7
N= 8
N= 9
BZ-2
BZ-1
IA
CV
200 µm
c
BZ-2
BZ-1
IA
Medaka
Zebrafish
7 dpi
14 dpi
d
**
0.055
*
*
PODXL-2+ Area MK (%)
IA
BZ-1
BZ-2
7 dpi
14 dpi
60 dpi
e
ZF
MK
*
***
PODXL-2+ Area IA (%)
7 dpi
14 dpi

Figure 5: Differences in blood vessel formation between Zebrafish and Medaka after cardiac cryoinjury

a Representative images of AP-stained whole hearts from uninjured and cryoinjured (7, 14, 30, 60 and 120 dpi) Zebrafish and Medaka. Whole heart images: 4x; zoomed in apex: 8x objective. Sample sizes (N) are shown within panels. **b** Representative confocal maximal projection images of cryoinjured Zebrafish (7 and 14 dpi) and Medaka (7, 14 and 60 dpi) hearts immunostained for PODXL-2 (endothelial blood vessel surface, green), MHC (myocardium, magenta) and DAPI counterstained nuclei (blue). Images were adjusted similarly as described in Methods. The PODXL-2+ segmented areas are outlined in yellow. White dashed lines separate the three distinct regions analyzed, namely IA, injury, BZ-1 (first 100 µm of healthy myocardium adjacent to the IA) and BZ-2 (following 100 µm of healthy myocardium adjacent to BZ-1). Group sample sizes (N) are shown within panels. Scale bars, 200 µm. For 60 dpi, additional zoomed in views of merged and separate channels are shown, highlighting with yellow arrows PODXL-2+ vessel-like structures around the IA. Scale bars, 100 µm. **c** Zoomed view of PODXL-2+ blood vessel-like structures at the IA, BZ-1 and BZ-2 areas from Zebrafish and Medaka hearts at 7 and 14 dpi. Scale bars, 100 µm. **d** Quantification PODXL-2+ blood vessel area normalized by each region of interest (IA, BZ-1 and BZ-2) in Medaka at 7, 14 and 60 dpi. Each dot represents one biological replicate. Statistical differences were analyzed by Two-way ANOVA of matched values (IA, BZ-1 and BZ-2 from each heart) with Bonferroni's correction. **e** Comparison of the percentage of PODXL-2+ in Zebrafish (blue) and Medaka (red) at 7 and 14 dpi. Two-way ANOVA. $p < 0.1$ (number); *$p < 0.05$; **$p < 0.01$; ***$p < 0.001$. BZ-1, border zone 1; BZ-2, border zone 2; CV, coronary vessels; dpi, days postinjury; IA, injured area; MK, Medaka.

Cardiac function recovery after a CI is not universal among all Medaka fish, yet the cardiac function depletion does not affect the fish's swimming performance

As a final step during regeneration, the regenerating myocardium needs to be electrically coupled to the preserved tissue and cardiac function needs to be recovered. This occurs to a large extent in the Zebrafish heart regeneration[11]. Consequently, we sought to study if cardiomyocyte proliferation and reduction of the fibrotic tissue correlated with the recovery of the cardiac function also in Medaka. To that end, Medaka's cardiac function was evaluated longitudinally by echocardiography at basal conditions, prior to CI, and at 6, 14 and 130 dpi. In parallel, an uninjured group was imaged at the same time points. To confirm CI, we collected hearts from a subset of the CI Medaka group at 6 dpi and processed them for AFOG staining (Figure 6a). Echocardiography videos can be found in Supplementary Figure 6.

In hearts from the CI group, but not in the uninjured control group, there was an apically located akinetic ventricular wall area at 6 and 14 dpi. Such an area was no longer visible at 130 dpi (Figure S6). While there was a high intra-individual variability, no significant differences could be observed in the mean Fractional Shortening (FS) values comparing the different time points in the uninjured controls (Figure

6b). In the cryoinjured group, we observed a drop of the mean FS at 6 dpi ($p=0.114$) that reached statistical significance at 14 dpi. At 130 dpi, the FS values did not differ significantly compared to basal levels any longer (Figure 6c). Notably however, diverse cardiac response dynamics could be observed among cryoinjured individuals. We grouped animals into those in which the FS was not decreased in response to CI (N=2/15), those in which there was no recovery of the FS (6/14 dpi FS ≥ 130 dpi FS) (N=4/13), those that recovered FS partially (6/14 dpi FS < 130 dpi FS < basal levels FS) (N=5/13) and finally, those revealing full FS recovery (130 dpi FS ≥ basal FS) (N=4/13). Overall, 9 out of 13 Medaka (≈70%), that displayed a reduction of FS at 6/14 dpi had fully or partially recovered FS, resulting in an average FS increase of 45% of their basal levels by 130 dpi (Figure 6b-d).

After intravital imaging, hearts were extracted at 130 dpi. Overall, whole mounted hearts showed a more rounded morphology, losing the pointed shape and small invaginations appeared with the resolution of the injury as seen before (Figure 6e). Interestingly, independently of their FS recovery status the IA was in all cases significantly smaller when compared to 6 dpi CI controls (Figure 6e and f). However, dense collagen aggregates at the ventricular apex could be seen within all CI groups (no FS recovery, partial FS recovery and full FS recovery) (Figure 6e). The wound was closed in 3/15 hearts at 130 dpi (Figure 7a). In most cases the fibrotic plaque was positioned very apically and thus seemed to be extruded outwards rather than being engulfed. This was particularly noticeable in the heart with the biggest injury (Figure 7b and c). Overall, we observed evidence of cardiac function recovery in Medaka, that did not fully correlate with the level of fibrotic tissue regression.

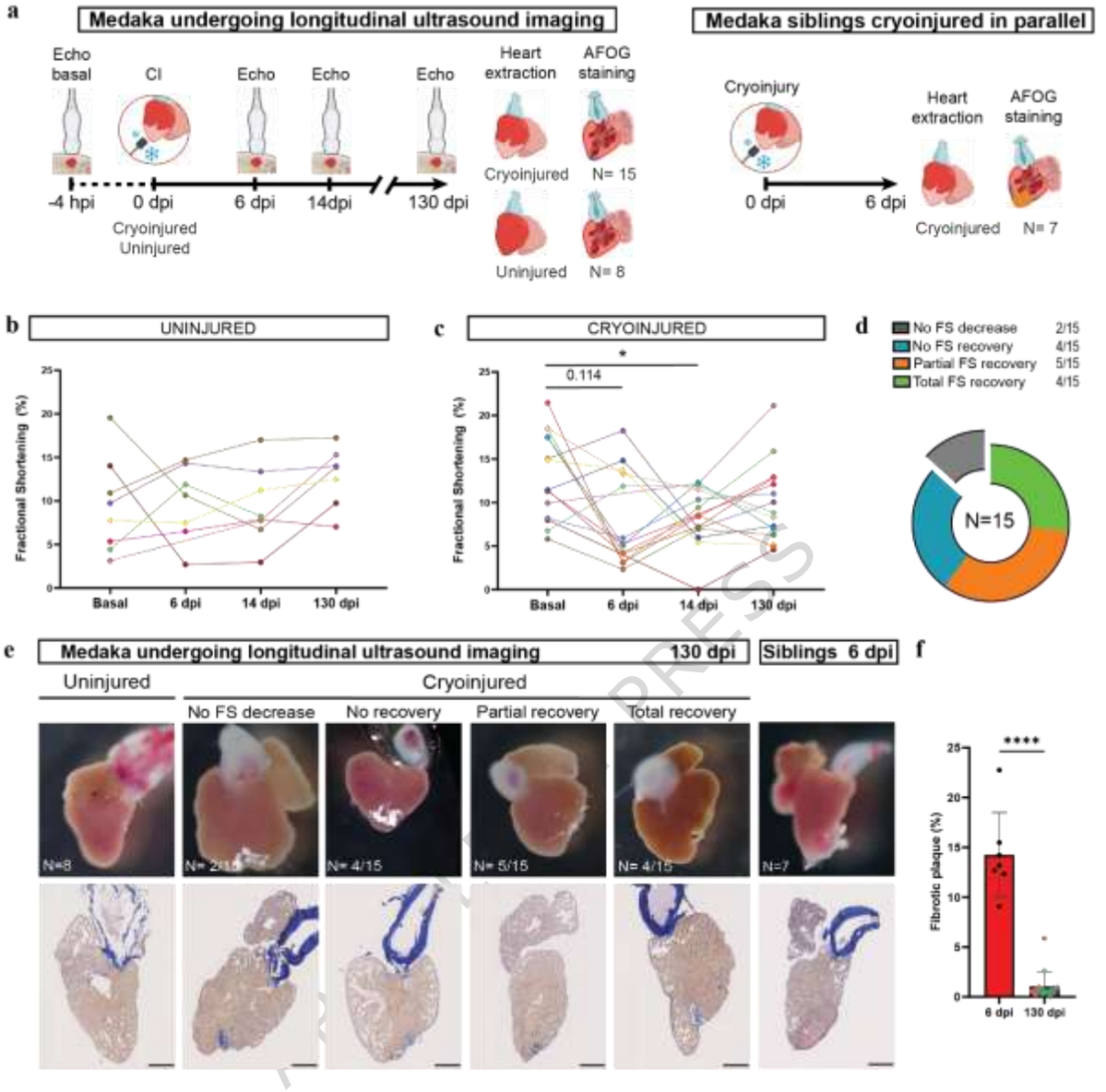

Figure 6: Echocardiographic evaluation of the regenerating heart in Medaka

a Schematic representation of the echocardiography experimental design. Cardiac function was analyzed in basal conditions. Later that day, fish were divided into two groups: cryoinjured and uninjured (control), and the cardiac function was longitudinally evaluated at 6, 14 and 130 days. At the endpoint, hearts were processed for AFOG staining to measure the fibrotic plaque area. As control that cryoinjuries were efficient, a parallel group of Medaka were cryoinjured and their hearts processed for AFOG at 6 dpi. Images were created with BioRender. **b and c** Echocardiography quantifications of FS (%) at basal conditions, 6, 14 and 130 days from uninjured (b) and cryoinjured (c) Medaka. Each individual is represented by a different color. Paired One-Way ANOVA mixed model. **d** Pie chart of the cryoinjured individuals based on their FS longitudinal status: No FS decrease (gray), No recovery (blue), Partial recovery (orange) and Total recovery (green). Group sample sizes (N) are shown. **e** Whole heart images: 4x objective (top), and AFOG (bottom) stained heart sections (blue: collagen, orange: fibrin, brown: myocardium) from the echocardiography-analyzed Medaka (130 dpi) and siblings cryoinjured in parallel

(6 dpi). Scale bars, 250 µm. Group sample sizes (N) are shown. **f** Quantification of the fibrotic plaque (%) in CI Medaka at 6 dpi and CI echocardiography analyzed Medaka at 130 dpi CI whole hearts. Shown are individual fish measurements as well as means ± S.D. 130 dpi individuals are colored based on their FS status shown in (d). Unpaired t-test. $p < 0.15$ (number); *$p < 0.05$; ****$p < 0.0001$. dpi, days postinjury; FS, fractional shortening.

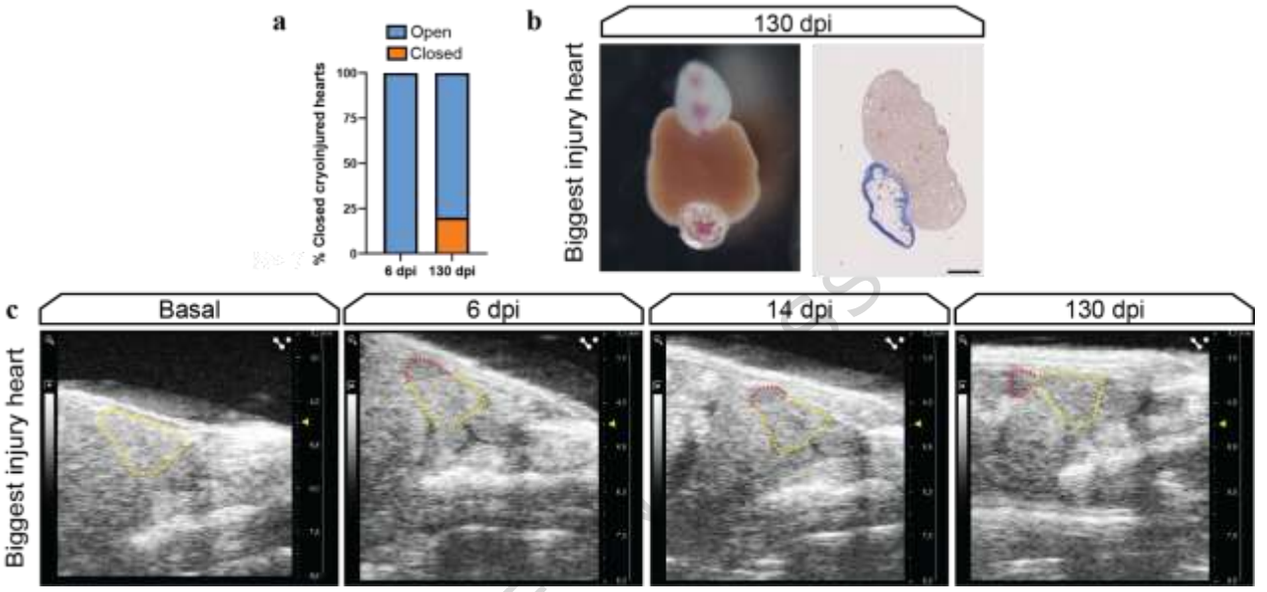

Figure 7: Echocardiographic and histological analysis show deficient injury engulfment during Medaka heart regeneration.

a Bar plot representation of open (blue) versus closed (orange) hearts (%) in CI Medaka at 6 dpi and CI echocardiography analyzed Medaka at 130 dpi. Chi-square test. No significant differences were detected. **b** Whole heart image: 4x objective (left), and AFOG (right) stained heart section (blue: collagen, orange: fibrin, brown: myocardium) from the echocardiography analyzed Medaka fish with the biggest injury. Scale bars, 250 µm. **c** 2D echocardiography images from the fish shown in (b) longitudinally evaluated at basal condition, 6, 14 and 130 dpi. The ventricular wall is outlined with a dashed yellow line, and the akinetic region marking the injury is outlined in red. dpi, days post injury.

Finally, we assessed swimming performance to gain a better understanding of how heart dysfunction after a CI might affect physical condition as a whole. The U_{crit}, defined as the maximum water flow a fish can swim against (Figure 8a), was measured at 7, 30 and 60 dpi to address whether the response to a heart injury of Zebrafish and Medaka may affect their swimming capacity. We found significant differences in the overall swimming performance between Zebrafish and Medaka. However, no significant differences could be observed between cryoinjured and uninjured groups in either teleost species at the time points analyzed (Figure 8b). Thus, despite a transient drop in cardiac function Medaka's swimming performance is not altered during the regeneration process.

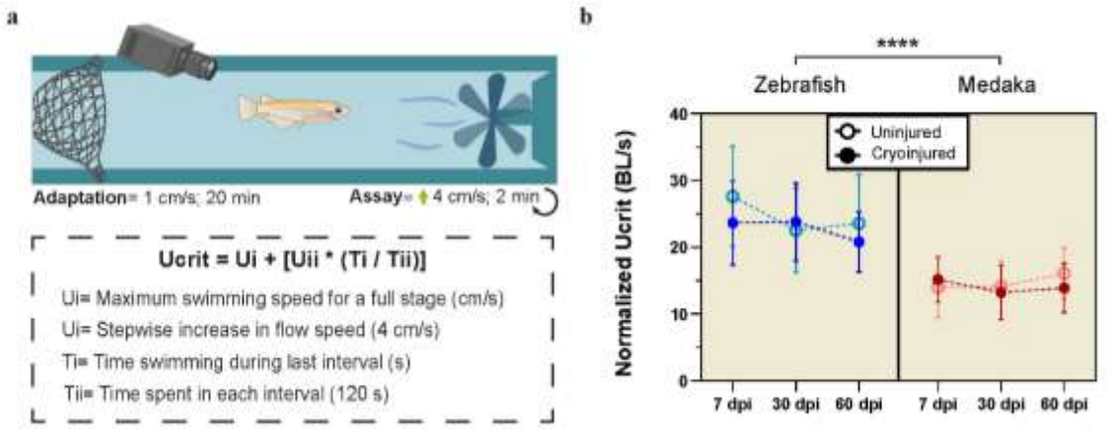

Figure 8: Cardiac cryoinjury does not impair swimming performance in Zebrafish and Medaka

a Schematic representation of the swimming performance assay. An adaptation period of 20 minutes at 1 cm/s was followed by the experimental assay, consisting of a stepwise swimming speed increase of 4 cm/s every 2 minutes. The experiment stopped when the fish fell to the net and maximum swimming speed (U_{crit}) was calculated following the shown equation. Images created with BioRender **b** Statistical analysis of swimming performance after a cryoinjury (7, 30 and 60 dpi) in Zebrafish (blue, N= 7) and Medaka (red, N= 8 at 7 and 30 dpi; N=7 at 60 dpi). Uninjured fish (white circle outlined with blue, Zebrafish; or red, Medaka) were evaluated simultaneously as control. U_{crit} values were normalized by the fish's body length (BL; in cm). Shown are means ± S.D. Three-way ANOVA with Bonferroni's correction. ****p <0.0001. dpi, days postinjury.

DISCUSSION

In contrast to Zebrafish, Medaka is considered a cardiac non-regenerative teleost[12,20]. However, while some comparative studies have been reported[13,15,16], a thorough comparative analysis englobing different stages of heart regeneration in Zebrafish and Medaka had not been reported yet. Our results show that, in contrast to the current paradigm, Medaka do not completely lack a regenerative response.

Contrary to the results obtained with a ventricular resection model[13], we observed a significant increase in cardiomyocyte proliferation at 7 dpi after a CI in Medaka. However, the proliferative response was reduced compared to Zebrafish. The differential responses of heart resection and CI may be influencing the different dynamics of immune cell recruitment[21] or the proliferative status of cardiomyocytes, as has been suggested to occur in Zebrafish[22]. Alternatively, given that the previous report did not discern between BZ and whole ventricle, the increased proliferation at the BZ might have gone unnoticed. Additionally, the IA+BZ proliferative response of other cell types including endocardial cells, were similar between both species supporting that the overall proliferative response in Medaka follows a similar spatio-temporal pattern to that of Zebrafish. Nevertheless, we found a significant delay in EC colonization of the IA in Medaka, which correlates with the delay in the activation of migratory-related

transcriptional pathways observed before[15].

Apart from the differences in EC proliferation and IA colonization, we also observed alterations in their injury-induced blood vessel response. Medaka's ventricles lacked the coronary structure of Zebrafish. However, endocardial cell density within the ventricle was much higher in Medaka, most probably being evolutionary required to replace the presence of big coronary arteries and support the myocardial tissue[23]. Nevertheless, Medaka hearts retain the ability to induce blood vessel formation after injury, although this process is reduced and constitutionally different than that of Zebrafish. After a CI, while in Zebrafish new blood vessels originated from pre-existing coronary arteries, abnormal blood vessel structures emerged in Medaka's IA, being able to expand even outside of the damaged tissue. These vessel-like structures were, however, transient and the original irrigation pattern was restored in the regenerated tissue, hence resembling the resolution of auxiliary blood vessels needed for regeneration that can be seen in other healing processes[24]. While a vasculature network might not be necessary in Medaka uninjured conditions, these transient structures might serve as scaffold to support cardiomyocyte colonization of the injury area during regeneration as shown for Zebrafish[4]. Noteworthy, the cellular origin of Medaka's injury-derived vessel structures is yet to be described, as their formation could involve angiogenesis from internal endothelial cells, invasion of blood vessels from peripheral tissues, such as the pericardium which attaches tightly to the injury, or *de novo* vasculogenesis, although this process is uncommon in adulthood. Thus, a more thorough analysis is needed to determine the source of these transient vessel sprouts, and the mechanism behind the vasculature remodeling at later stages.

One important difference between Medaka and Zebrafish injury response was related to fibrosis. We observed alterations in fibrotic tissue deposition and regression dynamics as well as differences in ECM organization. Fibrin levels were higher and more diffuse throughout the injury in Medaka than Zebrafish at 7 dpi, and at 14 dpi still covered almost completely the IA. This could imply a higher fibrin deposition rate or a reduction in fibrinolysis. Indeed, fibrinolysis is a key step during heart regeneration[25,26]. Thus, the slow fibrinolysis rate suggested for Medaka may be a mechanism involved in the reduced CM proliferative response. On the other hand, reduced levels of collagen were seen in Medaka at 7 dpi, which is in agreement with its muted expression at that time point[16]. A delayed deposition might be, at least partially, a consequence of reduced macrophage recruitment observed in Medaka (this work and Lai *et al.*,[15]), as these immune cells actively participate in this process[27]. Importantly, not only the dynamics, but also the spatial ECM distribution was different among both species. Collagen was mostly found in the external part of Medaka's injury, away from the myocardium, contrary to Zebrafish. The ECM works as a network in which several collagen isoforms and other ECM proteins interact among each other and through cell-ECM interactions to orchestrate the heart's regeneration[28], and thus differences in its distribution can alter this process. For example, the ECM component Emilin2a regulates EC migration during Zebrafish heart regeneration[29], yet it is not significantly upregulated in Medaka after cryoinjury[16]. Thus, the delayed EC colonization of the IA could be a consequence of the different ECM dynamics observed. Finally, given that collagen remodeling affects CM invasion of the IA[27], the distal localization

of collagen in Medaka may impair myocardial expansion at the early stages of the injury.

Apart from spatial differences in early ECM deposition, our results also reveal a significant, but yet delayed and/or reduced, fibrotic plaque regression in Medaka compared to Zebrafish, in contrast to previous reports[13]. In particular, injuries of less than $^{1}/_{10}$ of the whole ventricle area at 7 dpi could regenerate efficiently. However, in larger lesions of up to $^{1}/_{5}$ of the ventricular area, a small but compact collagen aggregate persisted in most Medaka hearts even at time points ≥120 dpi. Nevertheless, this does not imply an absence of regeneration, as overall the fibrotic plaque was significantly reduced after larger lesions as well. Of note, our results showing that even Zebrafish are in some cases not fully regenerative are also in agreement with previous reports[10]. However, the number of incompletely regenerated hearts was much lower in Zebrafish than in Medaka. We noticed as well that unlike Zebrafish, in which the fibrotic tissue is mostly engulfed by cortical myocardium (leading to a closed wound phenotype), the collagen remnants were more often found in the open wound outside of the ventricle in Medaka. This could indicate that fibrotic tissue extrusion might be a mechanism operating in Medaka as observed in the longitudinal echocardiography analyses, which may be a direct consequence of their thinner cortical layer[16]. One of the main differences between Zebrafish and Medaka are alterations in the immune response, in particular a dampened macrophage infiltration (this work and Lai *et al*[15]). Given that macrophages are crucial for fibrotic tissue remodeling and regression, and also provide key signals involved in CM proliferation and revascularization[30], they are most probably one of the main reasons for the observed differences in tissular regeneration among both teleost species, as stated before[14].

Further explanations might be related to differences in quantifying fibrosis. Noteworthy, our staining distinguishes collagen and fibrin. Collagen deposition is delayed and most fibrotic tissue regression occurs while the majority of the injury is covered in fibrin, yet the previously stated lack of fibrosis regression after ventricular resection was quantified only based on collagen[13]. Besides, other experimental differences could be leading to the inconsistent injury responses, such as the signaling pathways activated depending of the injury model (ventricular resection[13] vs cryolesion) which for instance can affect lymphangiogenesis[31], or the animal's age, which can affect the immune response at the organism level [32]. Nonetheless, our results are in agreement with the overall persisting collagen deposits observed even at late stages of the injury resolution. Intriguingly, small invaginations appeared where the cryoinjury was induced specially after large injuries. This could suggest that CM invasion of the injury is impaired (as implied by the differential ECM organization) or that the reduced CM proliferation is not enough to restore basal levels. In conclusion, the cardiac regeneration processes are present in Medaka, but delayed (EC migration, fibrosis deposition and regression) and/or reduced (macrophage recruitment, cardiomyocyte proliferation, injury engulfment and blood vessel formation), resulting in a regenerative response that, although sufficient to resolve most of the fibrotic scar, can be incomplete.

Finally, we aimed to not only characterize tissular regeneration but also assess functional recovery after

CI in the Medaka species. Echocardiographic evaluation of the regenerating Medaka heart allowed to longitudinally observe a significant remodeling of the damaged myocardial wall as shown for Zebrafish[11]. However, despite a similar reduction of the fibrotic plaque, the recovery of the FS was not homogeneous, and not all fish were able to completely restore FS basal levels. Nevertheless, the cardiac function is at least partially restored in 70% of cryoinjured Medaka. Interestingly, despite the high short-term mortality and, most of the times, incomplete cardiac function recovery, the CI did not affect Medaka's swimming performance, similar to what was shown to happen in Zebrafish after CI[33]. These results suggest that Medaka are, at least to some extent, also able to regenerate their heart at the functional level without affecting the fish's physical performance.

Heart regeneration in teleost species is not exclusive of Zebrafish, since it has been described as well in Giant Danio (*Devario aequipinnatus*)[34] and Goldfish (*Carassius auratus*)[35]. Moreover, Medaka's cardiac regeneration potential shown in this work highlights a more widespread cardiac regeneration ability in the teleost species than previously thought. Therefore, it would be of interest to analyze other Medaka strains to further evaluate the conservation of the heart regeneration capacity in this family. The Cab strain used in this study had been held inbred for over 10 years. It is therefore possible that while the Medaka strain used in both this work and the literature is Cab Medaka, the accumulation of genetic variants caused by genetic drift or differences between the facilities could be affecting the regenerative response. In fact, a recent study has shown that wild-type Zebrafish strains regenerate differently depending on their metabolic reprogramming capacity during the cardiac injury response[36], providing further evidence that naturally occurring divergence can influence cardiac regeneration among the same species. Additionally, it is possible that unknown environmental variables might influence the regenerative capacity seen in this work, which may be of interest as well for future studies. In conclusion, the Medaka fish is able to regenerate a significant part of its heart after a CI through a process that, although delayed/reduced, resembles the heart regeneration hallmarks observed in Zebrafish. However, the regenerative capacity of Medaka may not be sufficient to completely resolve large injuries, leading to the persistence of small fibrotic scars and changes in cardiac function and morphology.

METHODS

Table 1 indicates reagents and equipment used.

REAGENT or RESOURCE	SOURCE	IDENTIFIER
Antibodies		
Anti-BrdU mouse IgG1	Becton Dickinson	Cat#347580 RRID: AB_400326
Anti-MYH1E (MHC) mouse IgG2B	DSHB	Cat#MF20 RIDD: AB_2147781
Anti-ERG rabbit IgG	Abcam	Cat#EPR3864 RIDD: AB_92513
Anti-Mpx rabbit IgG	GeneTex	Cat#GTX128379 RIDD: AB_2885768
Anti-Col1a1a mouse IgG1	DSHB	Cat#SP1.D8 RIDD: AB_528438
Anti-Podocalyxin-2 (PODXL-2) rabbit IgG	Gift from Belting H.G.[19]	N/A
Goat anti-IgG1 mouse alexa 488	Invitrogen	Cat#A-21121 RIDD: AB_2535764
Goat anti-rabbit alexa 488	Invitrogen	Cat#A-11008 RIDD: AB_143165
Goat anti-IgG2B mouse alexa 647	Invitrogen	Cat#A-21242 RIDD: AB_2535811
Goat biotin-SP-conjugated anti-rabbit	Jackson ImmunoResearch	Cat#111-065-003 RIDD: AB_2337959
Fluorocrome-Streptavidins	Jackson ImmunoResearch	N/A
Chemicals, peptides, and recombinant proteins		
Ethyl 3-aminobenzoate methanesulfonate (Tricaine)	Sigma-Aldrich	Cat#E10521
5-Bromo-2-deoxyuridine (BrdU)	Sigma-Aldrich	Cat#B5002-IG
Heparina sódica	Laboratorios Reig Jofré S.A.	608737.4
16% Paraformaldehyde acqueous solution	Electron Microscopy Sciences	Cat#15710

Tyramides	TSA Research Reagents	Cat#SAT701001EA
4',6-Diamidino-2-phenylindole (DAPI)	Sigma-Aldrich	Cat#D9542
Isolectin B4- Biotinilated	Vector	RIDD: B-1205-.5
FluorSave Reagent	Millipore	Cat#345789
NBT/BCIP solution	Roche Applied Science	Cat#11681451001
Isofluorane 250 ml	Ecuphar	N/A
Experimental models: Organisms/strains		
Zebrafish: AB	ZIRC	ZDB-ALT-230106-4
Medaka: Cab	Paola Bovolenta	N/A
Software and algorithms		
Fiji/ImageJ	NIH	RRID: SCR 002285
GraphPad Prism 10	GraphPad Software	N/A
NDP.view 2	Hamamatsu	U12388-01
VEVO2100 Imaging System	FUJIFILM VisualSonics	N/A
Other		
Swimming tunnel (5L/230V/50Hz)	Loligo Systems	Cat#SW10050

Table 1. Key Ressource Table.

Animal husbandry

Experiments were conducted with AB *Danio rerio* (Zebrafish) and Cab *Oryzias latipes* (Medaka) of 12-20 months of age (Table 1), except for the Medaka used in the echocardiography analysis that were 7-months-old when the CI was performed and hearts were extracted at 11-months-old. Animals were housed and experiments performed in accordance with Spanish bioethical regulations for the use of laboratory animals. Zebrafish and Medaka were maintained at a density of 6 and 3 fish/l respectively. Both species were raised in similar housing conditions of 28ºC water temperature, pH 7.5, conductivity of 550-650 µS/cm^2, 10% water exchange per day and 14/10 h light/dark cycles. Animals were fed twice a day. Fish's diet varied based on their age: living *Artemia nauplii* (until 2-month-old); SERA Micron

powder (until 1.5-month-old) and GEMMA Micro Skretting (from 1-month-old onwards). A more detailed description of the recirculating water system and metal/metalloid concentrations commonly found in the fish facility at CNIC can be found in[37]. Experimental procedures were approved by the Community of Madrid "Dirección General de Medio Ambiente" under the licensees PROEX 335.0/23 and PROEX 240.3/23 for Zebrafish and Medaka respectively. Euthanasia will be carried out by prolonged immersion of the animal in 0.032% Tricaine/MS-222 dissolved in system water (4 ml of 0.4% Tricaine stock in 50 ml of water), which will first induce sedation and then deep anesthesia due to anesthetic overdose. Once anesthetized, they will be transferred to water at 4°C to complete euthanasia.

Cardiac CI

CI was performed according to Gonzalez-Rosa *et al*. with little modifications[9]. Zebrafish and Medaka were anesthetized in pH-buffered 0.04% and 0.12% tricaine (Sigma) respectively. For generating the injury, the hand-made cryoprobe was cooled in liquid nitrogen and placed on the surface of the ventricle for no longer than 3 seconds. For sham operations, the pericardial sac was opened, and the heart was touched with a similar cryoprobe at room temperature (RT). The surgical material was sterilized with 70% ethanol between each operation. A step-by-step graphical representation of the process can be seen in Figure 1a.

Histology and immunohistochemistry on sections

For proliferation analysis, 20 µl of 2 mg/ml of 5-Bromo-2-deoxyuridine (BrdU, B5002-1G, Sigma) were injected intraperitoneally 24 hours prior to the heart extraction. Hearts were extracted and placed in phosphate-buffered saline (PBS) – 40 IU heparin (Laboratorios ROVI) to avoid the formation of blood clots until the fixation of the tissue. The hearts were then incubated in 100 mM KCl for 10 minutes and fixed overnight in 4% paraformaldehyde (PFA; Electron Microscopy Sciences) at 4ºC. Samples were paraffin or gelatin embedded and sectioned in 2-chamber longitudinal cuts at 7 µm or 8 µm width using a microtome or cryostat, respectively. Sections were included in 6 slides in a serial manner (section 1-3 slide 1, section 4-6 slide 2…) in a way that each slide has representation of the whole heart.

Paraffin sections were immunostained as described before[5] using the following primary antibodies: IgG1 Mouse anti-BrdU (1:100, B44, Becton Dickinson), IgG2B Mouse anti-MHC (1:20, MF20, DSHB), IgG Rabbit anti-ERG (1:100, EPR3863, Abcam), IgG Rabbit anti-Mpx (1:200, GTX128379, GeneTex) and Isolectin B4-biotinilated (1:200, B1205, Vector). For collagen analysis, cryosections were immunostained with the primary antibody IgG1 Mouse anti-Col1a1a (1:20, SP1.D8, DSHB) amplified with Tyramides (PerkinElmer). The secondary antibodies were used in a 1:250 concentration: Alexa488 goat anti-IgG1 Mouse (Invitrogen), Alexa 488 goat anti-rabbit (Invitrogen), Alexa647 goat anti- IgG2B Mouse (Invitrogen), and goat Biotin-SP-conjugated anti-rabbit (Jackson ImmunoResearch) conjugated with a Fluorocrome-Streptavidin (Jackson ImmunoResearch). Nuclei were counterstained with 4',6-Diamidino-2-phenylindole (DAPI). Images were taken with a Zeiss LSM 700 confocal microscope. The

same image acquisition method was used for all heart sections from each experiment, and brightness and contrast were manually adjusted on FIJI ImageJ software for proper visualization during quantification. For quantifications, ventricles were separated into 3 regions of interest: Injury Area (IA), defined as the ventricle MF20- area marking the lesion; Border Zone area (BZ), defined as the closest 100 µm of the ventricle to the IA; and the Periphery Area (PA). After manually annotating the IA, the BZ was obtained by enlarging the IA selection 100 µm with edit selection settings in FIJI software, and the area between the IA border and this last selection was analyzed for the BZ. In uninjured hearts the whole ventricle was analyzed. For proliferation analysis, the number of BrdU+ cells were normalized by the total number of each cell type (%) or area (in mm^2). For the analysis of endocardial cell colonization of the injury, the IA was segmented into 5 equidistant segments numbered from 1 (closest to the BZ) to 5 (furthest to the BZ) by a customized FIJI macro, and cell density was obtained by using StarDist automated cell counting plugin normalized by each section area.

One slide per heart was stained by AFOG[1]. For quantifications, all sections from the slide were analyzed as a representation of the total fibrotic tissue found in each heart. The fibrotic plaque: collagen (blue) and fibrin (orange); and healthy myocardium (beige) areas were annotated manually in each section in FIJI: ImageJ software. The scar size (fibrin + collagen) was normalized by the total ventricular area (fibrin + collagen + myocardium) in order to obtain the fibrotic plaque percentage of the whole heart. Additionally, AFOG stained sections were captured under a Leica 4 Tune-Dive-Stellaris8-Falcon multiphoton microscope which allowed for the visualization of the fibrin fibers in fluorescence. The IA was manually annotated on each heart section and the same fluorescence intensity threshold was used on all sections to quantify the fibrin area.

Whole mount immunostaining

For whole-heart immunofluorescence, hearts were fixed overnight at 4ºC in 2% PFA (Electron Microscopy Sciences), permeabilized in 0.3% PBS-Triton-X-100 (30 mins, in the dark), blocked 2 hours with blocking buffer (0.3% PBS-Triton-X-100, 5% goat serum), and incubated overnight at 4 ºC with primary antibodies IgG Rabbit anti-PODXL-2 (1:200, gift from H. G. Belting) and IgG2B Mouse anti-MHC (1:20, MF20, DSHB). After two 10 min and one 30 min wash in PBS the samples were incubated with secondary antibodies Alexa 488 goat anti-rabbit (1:500, Invitrogen), Alexa 647 goat anti-mouse IgG2B (1:250, Invitrogen) diluted in blocking buffer. Incubation was again overnight at 4 ºC. Incubation was followed by two PBS washes, 10 mins each. Finally, nuclei were counterstained with DAPI (1:1000). Hearts were embedded in 2% low melting agarose (Sigma). Z-stack confocal images from the ventricular surface were captured under a Leica 4 Tune-Dive-Stellaris8-Falcon multiphoton microscope using a 5x objective for all hearts, and a 25x objective for 60 dpi zoomed in view. Maximal projections were processed in FIJI using a Macro to ensure proper identification of PODXL-2 structures: enhance contrast (saturated= 0.35 normalize), subtract background (rolling= 50), median (radius= 2) and enhance local contrast (blocksize=400, histogram 256, maximum=3). Three regions of interest were analyzed: IA,

injury; BZ-1, first 100 µm of healthy myocardium closer to the IA; and BZ-2, following 100 µm of healthy myocardium closer to the BZ-1. Selections were obtained based on MaxEntropy dark auto threshold. Manual corrections of the given selections were performed to ensure the inclusion of all vessel area. An example of the selections obtained can be found in Figure 5b. The selection area was normalized for each region of interest area to obtain the % of blood vessel occupancy.

Whole heart alkaline phosphatase staining

AP staining was performed in uninjured and cryoinjured hearts similar to Lai *et al.,*[15]. Briefly, after fixing (PFA, 1 hour, RT) and washing (PBS, 3x 10 min, RT), the hearts were equilibrated for 20 minutes in alkaline buffer (100 mM Tris, pH 9.5, 100 mM NaCl, 0.1% Tween20), followed by the addition of 1:100 NBT/BCIP solution (Roche Applied Science) to start the reaction. Once blue vessels could be observed under the microscope, hearts were washed (PBS, 3x 10 min, RT) and imaged.

Maximum swimming capacity assay

Maximum swimming speed was assessed individually in untrained fish in a 5L swimming performance tunnel (Loligo Systems Swim tunnel; 5L/230V/50Hz) similar to García-Poyatos *et al.,*[38]. To avoid sex variability, control and cryoinjured groups were established with the same number of fish and male-female ratio for each time point. The water temperature was maintained at 26–28ºC, ambient light was kept low to avoid distractions, and the tunnel was cleaned and the water renewed every day during the assay. Fish were first allowed to acclimatize for 20 minutes at 1 cm/s flow velocity in the swimming tunnel chamber. After adaptation, the current was increased in stages of 4 cm/s every 2 min. The assay stopped when the fish fell to the net and were not able to move for 3 seconds. The critical swimming speed (U_{crit}) was determined as: $U_{crit} = U_i + [U_{ii} * (T_i / T_{ii})]$, being U_i the maximum swimming speed (in cm/s) maintained for a full interval, U_{ii} the stepwise increase in the flow speed (4 cm/s), T_i the time (in seconds) spent swimming during the last interval and T_{ii} the total time spent in each stage (120 s). Maximum swimming values were normalized by the fish's body length (in cm).

Echocardiography

Medaka's cardiac function was longitudinally evaluated before and after a cardiac CI, as described before[11]. A group of uninjured fish was simultaneously analyzed as control, and the echocardiography was performed in a blind manner. Fish were anesthetized in a mix of 180 mM Tricaine (Sigma) and 4.5 mM Isoflurane (Baxter) in fish water until no movement could be observed. Once anesthetized, individual fish were placed ventral side up on a customized sponge and transferred into a petri dish with the anesthetic solution. The echocardiography videos were taken with a MS-700 (50 MHz) scan head (VisualSonics) and visualized with the Vevo2100 Imaging System. Fish were rotated as needed until proper visualization of the ventricle was achieved. Finally, fish were reanimated by pipetting fresh water onto the gills and were put back in individual fish tanks to be able to follow each fish's cardiac function

over time.

Statistical analysis

Statistical analyses were performed using GraphPad Prim v10 Software. Normal distribution was tested to decide if a parametric or non-parametric test needed to be applied. The statistical test used for each experiment and sample sizes are shown in figure legends. P-values below 0.05 were considered statistically significant. The significance levels are indicated in figures based on the number of asterisks, where: P < 0.1 (number); *P < 0.05; **P < 0.01; ***P < 0.001 and ****P< 0.0001. In each graph, different representation settings were used according to the data for proper visualization, in which the heigh of the bar represents the mean of each group, the standard deviation is shown as error bars and the value obtained for each biological replicate is represented as an individual dot.

DATA AVAILABILITY

Raw data related to this manuscript have been deposited at Zenodo under accession number **10.5281/zenodo.18228803**.

ACKNOWLEDGEMENTS

We thank Eduardo Díaz for excellent Zebrafish and Medaka husbandry at the CNIC Animal Facility and Paola Bovolenta for sharing the Cab Medaka line. We thank Jochen Wittbrodt and Felix Loosli, for discussion. We thank Heinz-Georg Belting for sharing the PODXL-2 antibody. Finally, we thank the Histopathology team from CNIC Comparative Medicine Unit for support on sample processing, the CNIC Microscopy and Dynamic Imaging Unit for excepcional assistance on image adquisition and analysis, and the Advanced Imaging Unit at CNIC for the echocardiography analysis, in particular Lorena Flores and Ana Vanesa Alonso. The Microscopy Unit at CNIC obtained the grant EQC2021-007527-P funded by MCIN/AEI/10.13039/501100011033 and by the European Union NextGenerationEU/PRTR. The Advanced Imaging Unit at CNIC obtained funding for the imaging analysis VEVO system (grant EQC2024-008109-P) by MICIU/AEI /10.13039/501100011033 and ERDF, EU. This work was supported by the European Union's Horizon 2020 research and innovation programme under grant agreements No 819717 (N.M.) and 819719 (M.T.) The CNIC is supported by the Instituto de Salud Carlos III (ISCIII), the Spanish Ministry of Science, Innovation and Universities, and the Pro CNIC Foundation and is a Severo Ochoa Center of Excellence (CEX2020-001041-S financed by MICIN/AEI/10.13039/501100011033).

AUTHOR CONTRIBUTIONS

Conceptualization: N.M. and M.T. Funding acquisition: N.M. and MT. Experimentation and Statistical analysis: M.A.G and M.G.C. Supervision: N.M. and M.T. Writing – original draft: M.A.G., N.M., and M.T. Writing – review: M.A.G., M.G.C., N.M. and M.T.

COMPETING INTERESTS

The authors declare no competing financial or non-financial interests.

ADDITIONAL INFORMATION

Supplementary information: The online version contains supplementary material available at

Correspondence and requests for materials should be addressed to Nadia Mercader.

REFERENCES

1 Poss, K. D., Wilson, L. G. & Keating, M. T. Heart regeneration in zebrafish. *Science* **298**, 2188-2190, doi:10.1126/science.1077857 (2002).

2 Sanz-Morejon, A. & Mercader, N. Recent insights into zebrafish cardiac regeneration. *Curr Opin Genet Dev* **64**, 37-43, doi:10.1016/j.gde.2020.05.020 (2020).

3 Ross Stewart, K. M., Walker, S. L., Baker, A. H., Riley, P. R. & Brittan, M. Hooked on heart regeneration: the zebrafish guide to recovery. *Cardiovasc Res* **118**, 1667-1679, doi:10.1093/cvr/cvab214 (2022).

4 Marin-Juez, R. *et al.* Coronary Revascularization During Heart Regeneration Is Regulated by Epicardial and Endocardial Cues and Forms a Scaffold for Cardiomyocyte Repopulation. *Dev Cell* **51**, 503-515 e504, doi:10.1016/j.devcel.2019.10.019 (2019).

5 Sanchez-Iranzo, H. *et al.* Transient fibrosis resolves via fibroblast inactivation in the regenerating zebrafish heart. *Proc Natl Acad Sci U S A* **115**, 4188-4193, doi:10.1073/pnas.1716713115 (2018).

6 Marin-Juez, R. *et al.* Fast revascularization of the injured area is essential to support zebrafish heart regeneration. *Proc Natl Acad Sci U S A* **113**, 11237-11242, doi:10.1073/pnas.1605431113 (2016).

7 Jopling, C. *et al.* Zebrafish heart regeneration occurs by cardiomyocyte dedifferentiation and proliferation. *Nature* **464**, 606-609, doi:10.1038/nature08899 (2010).

8 Honkoop, H. *et al.* Single-cell analysis uncovers that metabolic reprogramming by ErbB2 signaling is essential for cardiomyocyte proliferation in the regenerating heart. *Elife* **8**, doi:10.7554/eLife.50163 (2019).

9 Gonzalez-Rosa, J. M., Martin, V., Peralta, M., Torres, M. & Mercader, N. Extensive scar formation and regression during heart regeneration after cryoinjury in zebrafish. *Development* **138**, 1663-1674, doi:10.1242/dev.060897 (2011).

10 Bertozzi, A. *et al.* Is zebrafish heart regeneration "complete"? Lineage-restricted cardiomyocytes proliferate to pre-injury numbers but some fail to differentiate in fibrotic hearts. *Dev Biol* **471**, 106-118, doi:10.1016/j.ydbio.2020.12.004 (2021).

11 Gonzalez-Rosa, J. M. *et al.* Use of echocardiography reveals reestablishment of ventricular pumping efficiency and partial ventricular wall motion recovery upon ventricular cryoinjury in the zebrafish. *PLoS One* **9**, e115604, doi:10.1371/journal.pone.0115604 (2014).

12 Chowdhury, K., Lin, S. & Lai, S. L. Comparative Study in Zebrafish and Medaka Unravels the Mechanisms of Tissue Regeneration. *Front. Ecol. Evol* **10**, doi:10.3389/fevo.2022.783818 (2022).

13 Ito, K. *et al.* Differential reparative phenotypes between zebrafish and medaka after cardiac injury. *Dev Dyn* **243**, 1106-1115, doi:10.1002/dvdy.24154 (2014).

14 Lai, S. L., Marin-Juez, R. & Stainier, D. Y. R. Immune responses in cardiac repair and regeneration: a comparative point of view. *Cell Mol Life Sci* **76**, 1365-1380, doi:10.1007/s00018-018-2995-5 (2019).

15 Lai, S. L. *et al.* Reciprocal analyses in zebrafish and medaka reveal that harnessing the immune response promotes cardiac regeneration. *Elife* **6**, doi:10.7554/eLife.25605 (2017).

16 Carey, C. M., Hollins, H. L., Schmid, A. V. & Gagnon, J. A. Distinct features of the regenerating heart uncovered through comparative single-cell profiling. *Biol Open* **13**, doi:10.1242/bio.060156 (2024).

17 Chowdhury, K. *et al.* Immune modulation promotes heart regeneration through macrophage and Granulin functions in medaka. *Proc Natl Acad Sci U S A* **123**, e2524705123, doi:10.1073/pnas.2524705123 (2026).

18 Lemanski, L. F., Fitts, E. P. & Marx, B. S. Fine structure of the heart in the Japanese Medaka, Oryzias latipes. *J Ultrastruct Res* **53**, 37-65, doi:10.1016/s0022-5320(75)80085-2 (1975).

19 Herwig, L. *et al.* Distinct cellular mechanisms of blood vessel fusion in the zebrafish embryo. *Curr Biol* **21**, 1942-1948, doi:10.1016/j.cub.2011.10.016 (2011).

20 Potts, H. G., Stockdale, W. T. & Mommersteeg, M. T. M. Unlocking the Secrets of the Regenerating Fish Heart: Comparing Regenerative Models to Shed Light on Successful Regeneration. *J Cardiovasc Dev Dis* **8**, doi:10.3390/jcdd8010004 (2021).

21 Bevan, L. *et al.* Specific macrophage populations promote both cardiac scar deposition and subsequent resolution in adult zebrafish. *Cardiovasc Res* **116**, 1357-1371, doi:10.1093/cvr/cvz221 (2020).

22 Botos, M. A., Arora, P., Chouvardas, P. & Mercader, N. Transcriptomic data meta-analysis reveals common and injury model specific gene expression changes in the regenerating zebrafish heart. *Sci Rep* **13**, 5418, doi:10.1038/s41598-023-32272-6 (2023).

23 Farrell, A. P. & Steffensen, J. F. Coronary ligation reduces maximum sustained swimming speed in Chinook salmon, Oncorhynchus tshawytscha. *Comp Biochem Physiol A Comp Physiol* **87**, 35-37, doi:10.1016/0300-9629(87)90421-x (1987).

24 Wietecha, M. S., Cerny, W. L. & DiPietro, L. A. Mechanisms of vessel regression: toward an understanding of the resolution of angiogenesis. *Curr Top Microbiol Immunol* **367**, 3-32, doi:10.1007/82_2012_287 (2013).

25 Narumanchi, S. *et al.* Inhibition of let-7c Regulates Cardiac Regeneration after Cryoinjury in Adult Zebrafish. *J Cardiovasc Dev Dis* **6**, doi:10.3390/jcdd6020016 (2019).

26 Munch, J., Grivas, D., Gonzalez-Rajal, A., Torregrosa-Carrion, R. & de la Pompa, J. L. Notch signalling restricts inflammation and serpine1 expression in the dynamic endocardium of the regenerating zebrafish heart. *Development* **144**, 1425-1440, doi:10.1242/dev.143362 (2017).

27 Constanty, F. *et al.* Border-zone cardiomyocytes and macrophages regulate extracellular matrix remodeling to promote cardiomyocyte protrusion during cardiac regeneration. *Nat Commun* **16**, 3823, doi:10.1038/s41467-025-59169-4 (2025).

28 Wu, B., Constanty, F. & Beisaw, A. Cardiac regeneration: Unraveling the complex network of intercellular crosstalk. *Semin Cell Dev Biol* **171**, 103619, doi:10.1016/j.semcdb.2025.103619 (2025).

29 El-Sammak, H. *et al.* A Vegfc-Emilin2a-Cxcl8a Signaling Axis Required for Zebrafish Cardiac Regeneration. *Circ Res* **130**, 1014-1029, doi:10.1161/CIRCRESAHA.121.319929 (2022).

30 Byatt, T. C., Razaghi, E., Tuzuner, S. & Simoes, F. C. Immune-mediated cardiac development and regeneration. *Semin Cell Dev Biol* **171**, 103613, doi:10.1016/j.semcdb.2025.103613 (2025).

31 Harrison, M. R. *et al.* Late developing cardiac lymphatic vasculature supports adult zebrafish heart function and regeneration. *Elife* **8**, doi:10.7554/eLife.42762 (2019).

32 DiBona, E., Humble, J., Duran, D., Au, D. W. T. & Seemann, F. Characterization of Immune Aging in the Japanese Medaka (Oryzias latipes). *Fishes* **9 (9)**, 333, doi:10.3390/fishes9090333 (2024).

33 Rovira, M., Borras, D. M., Marques, I. J., Puig, C. & Planas, J. V. Physiological Responses to Swimming-Induced Exercise in the Adult Zebrafish Regenerating Heart. *Front Physiol* **9**, 1362, doi:10.3389/fphys.2018.01362 (2018).

34 Lafontant, P. J. *et al.* The giant danio (D. aequipinnatus) as a model of cardiac remodeling and regeneration. *Anat Rec (Hoboken)* **295**, 234-248, doi:10.1002/ar.21492 (2012).

35 Grivas, J. *et al.* Cardiac repair and regenerative potential in the goldfish (Carassius auratus) heart. *Comp Biochem Physiol C Toxicol Pharmacol* **163**, 14-23, doi:10.1016/j.cbpc.2014.02.002 (2014).

36 Lekkos, K. *et al.* Oxidative phosphorylation is required for cardiomyocyte re-differentiation and long-term fish heart regeneration. *Nat Cardiovasc Res* **4**, 1363-1380, doi:10.1038/s44161-025-00718-x (2025).

37 Langa, X. *et al.* A Systematic Analysis of Metal and Metalloid Concentrations in Eight Zebrafish Recirculating Water Systems. *Zebrafish* **18**, 252-264, doi:10.1089/zeb.2020.1970 (2021).

38 Garcia-Poyatos, C. *et al*. Cox7a1 controls skeletal muscle physiology and heart regeneration through complex IV dimerization. *Dev Cell* **59**, 1824-1841 e1810, doi:10.1016/j.devcel.2024.04.012 (2024).